

Influence of spin density in implanted Si layers on pulsed-laser annealing

K. Murakami, E. Ikawa, K. Gamo, and S. Namba

Faculty of Engineering Science, Osaka University, Toyonaka, Osaka 560, Japan

Y. Akasaka

LSI Development Laboratory, Mitsubishi Electric Corporation, Mizuhara, Itami, Japan

Y. Masuda

Faculty of Science, Osaka University, Toyonaka, Osaka, Japan

(Received 7 May 1979; accepted for publication 15 June 1979)

In order to clarify an influence of the spin density or the optical absorption coefficient on the pulsed-laser annealing effect, we have performed systematically ion-backscattering and channeling analysis and ESR measurement as a function of spin densities in ion-implanted Si samples. It was found that the spin density can yield a good criterion for predicting the annealing effect because the spin density is strongly correlated with the optical absorption coefficient. From spin-density measurements, the initial absorption coefficient of the as-implanted Si layer was found to be a very important factor which dominates the effect of laser annealing even if there is a nonlinear absorption mechanism.

PACS numbers: 61.70.Tm, 81.40.Ef

The effect of pulsed-laser annealing on ion-implanted Si has been studied by many workers.¹⁻⁹ However, they have not thoroughly made clear factors that dominate the annealing effect, although it was suggested by several workers that the effect depends on the kinds of implanted ions,³ the optical-absorption coefficient of the as-implanted layer,⁴⁻⁶ and the thickness of an amorphous layer.⁷ In this letter we report on experiments to clarify an influence of the initial spin density in the implanted layer on the subsequent annealing effect. The spin density N_s is strongly correlated with the absorption coefficient α , i.e., α increases with an increase of N_s since most localized states in the mobility gap or the forbidden gap of Si are originated from dangling bonds or unpaired electrons.^{10,11} Therefore, it is expected that N_s becomes a criterion to predict laser annealing effects.

Arsenic or phosphorus ions were implanted at room temperature. A description is given in Table I of the samples used in these experiments and of the condition of ion implantations. The implanted layers were made amorphous for some samples, but were heavily damaged crystalline for other samples. These samples were irradiated in air with four kinds of pulsed lasers which are described in Table II. The beam diameter of the Q-switched ruby laser was about 1.5

cm. For other lasers the samples were overlapping irradiated in a half-diameter pitch since the beam diameters were 1.4–2.5 mm.

The extent of the crystallization by laser annealing was determined by ion-backscattering and channeling analysis (RBS) using 2.0-MeV He⁺ ions and the electron-spin resonance (ESR). ESR measurements were performed at room temperature by using the microwave frequency of 9 GHz. Although various kinds of ESR centers are observed in the heavily damaged crystalline Si,¹² we measured only the total amount of spins. In the complete amorphous Si, only an isotropic ESR signal is observed at the g value of 2.006.² N_s of implanted layers was obtained by assuming that spins are uniformly distributed over a depth $2R_p$.¹³

Figure 1 shows the dependence of the crystalline-recovery ratio R on N_s of as-implanted Si. The R means an annealed fraction of spins or ESR centers, which roughly corresponds to the degree of crystallization or of annealing of total defects.¹² In the case of irradiations with both types of Nd:YAG laser at ~ 5 J/cm², the recovery ratio has a remarkably strong N_s dependence. On the other hand, the irradiation of the normal ruby laser at ~ 1 J/cm² shows a weak N_s dependence of the recovery, and the irradiation of

TABLE I. Samples used and condition of ion implantations.

Ion	Energy (keV)	Dose (cm ⁻²)	Ion current (μ A/cm ²)	Si substrate type, g.m. ^a , ρ (Ω cm), Surface
P	120	5×10^{15}	0.5	p , F.Z., 100–200, (111)
	100	1×10^{15} (3μ A/cm ²), 1×10^{16} (1μ A/cm ²)		p , C.Z., 1–2, (111)
	100	1×10^{14} , 3×10^{14} , 1×10^{15} , 1×10^{16}	1	p , C.Z., 10–20, (100)
	50	5×10^{15}	1	p , C.Z., 1–2, (111)
As	100	1×10^{14} , 1×10^{15} , 5×10^{15}	3	p , C.Z., 1–2, (111)
	100	1×10^{14} , 3×10^{14} , 1×10^{15} , 1×10^{16}	1	p , C.Z., 10–20, (100)

^aGrowth method.

TABLE II. Four kinds of pulsed lasers used in this study.

Pulsed laser	Mode	Pulse width (FWHM)	Wavelength
Q-switched ruby laser	Multi and single	30 nsec	0.69 μm
Normal ruby laser	Multi	100 μsec	0.69 μm
Q-switched Nd : YAG laser	Multi	20 nsec	1.06 μm
Mode-locked Nd : YAG laser	Single	pulse width of 30 psec, time separation of 10 nsec, and pulse-train duration of 150 nsec	1.06 μm

the Q-switched ruby at 1.6 J/cm^2 shows no N_s dependence and a nearly complete recovery. These results suggest that for a long wavelength of $1.06 \mu\text{m}$ the annealing effect is remarkably enhanced by the increase of N of the as-implanted Si layer.

Figure 2 shows the N_s dependence of χ_{\min} (Si) of laser annealed samples. χ_{\min} , which is the minimum yield in the channeling direction, is seen to decrease roughly with N_s , i.e., the crystalline recovery increases with N_s . Therefore, it is considered from these ESR measurements and RBS analysis that the spin density is a main factor which dominates the effect of the pulsed-laser annealing.

In order to further clarify the influence of spins on the annealing effect, we measured laser annealing effects for two kinds of amorphous Si made by an ion implantation (70-kV As + $3.5 \times 10^{15}/\text{cm}^2$). One is the as-implanted Si with a N_s of $6.3 \times 10^{19} \text{ spins/cm}^3$ and the other is the Si with a lower N_s of $3.4 \times 10^{19} \text{ spins/cm}^3$ which was annealed at 400°C for 15 min in the atmosphere of pure H_2 . The two Si samples were checked by RBS to have an equal thickness of amorphous layer. Then the samples were irradiated with a Q-switched ruby laser pulse of 0.4 J/cm^2 at which the complete crystallization is not induced.⁴ N_s was decreased by the laser

annealing from 6.3×10^{19} to $3.8 \times 10^{19} \text{ spins/cm}^3$ for the as-implanted Si and from 3.4×10^{19} to $2.6 \times 10^{19} \text{ spins/cm}^3$ for the thermally annealed Si. RBS results indicate, as shown in Fig. 3, that χ_{\min} of as-implanted Si and thermally annealed Si are 22.6 and 26.0%, respectively. This result was reproducible among two different spots on the same sample. It was found from these experiments that even with the Q-switched ruby-laser irradiation the crystalline recovery is better for the amorphous Si with higher N_s than that with lower N_s . RBS is not a good criterion for predicting laser annealing effects but spin density obtained by ESR measurements is a good one.

A positive feedback of temperature rise is very important for the laser annealing.^{2,6,8,9} The laser annealing mechanism contains three processes, i.e., (1) the optical-absorption process, (2) the relaxation process of the absorbed laser energy to thermal energy, and (3) the dissipation process of ther-

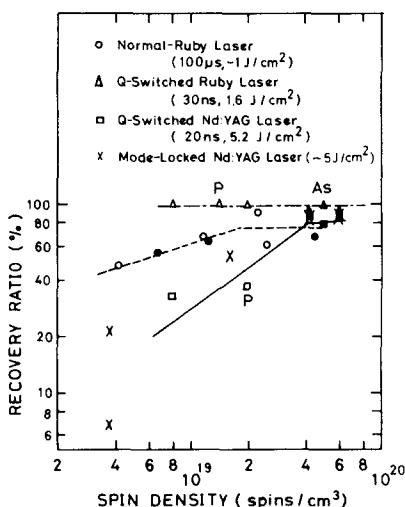


FIG. 1. Dependence of the crystalline-recovery ratio on the spin densities of as-implanted Si. Open and close signs indicate P- and As-implanted Si, respectively. \times signs at $4 \times 10^{19}/\text{cm}^3$ and $6 \times 10^{19}/\text{cm}^3$ indicate As-implanted Si; the other two \times signs indicate P-implanted Si.

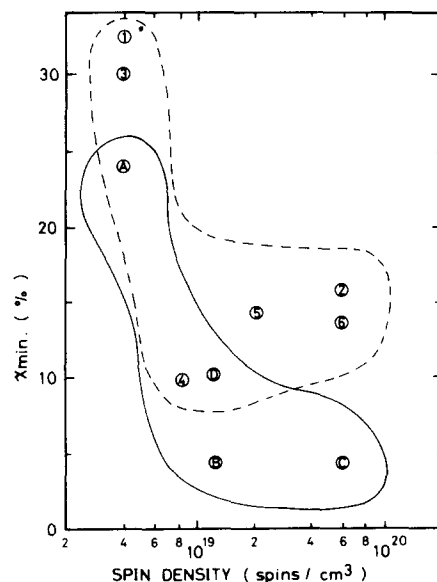


FIG. 2. N_s dependence of χ_{\min} (Si) of laser-annealed Si. 1–6 and A–D indicate Si samples as follows: 1 P + $1 \times 10^{16}/\text{cm}^2$, M-YAG $\sim 5 \text{ J/cm}^2$; 2 As + $1 \times 10^{15}/\text{cm}^2$, M-YAG $\sim 5 \text{ J/cm}^2$; 3 P + $1 \times 10^{16}/\text{cm}^2$, Q-YAG 5.2 J/cm^2 ; 4 P + $1 \times 10^{14}/\text{cm}^2$, Q-YAG 5.2 J/cm^2 ; 5 P + $3 \times 10^{14}/\text{cm}^2$, Q-YAG 5.2 J/cm^2 ; 6 As + $1 \times 10^{15}/\text{cm}^2$, Q-YAG 5.2 J/cm^2 ; A P + $1 \times 10^{16}/\text{cm}^2$, Q-ruby 0.6 J/cm^2 ; B As + $5 \times 10^{15}/\text{cm}^2$, Q-ruby 0.6 J/cm^2 ; C As + $1 \times 10^{15}/\text{cm}^2$, Q-ruby 1.6 J/cm^2 ; D As + $5 \times 10^{15}/\text{cm}^2$, N-ruby $\sim 1 \text{ J/cm}^2$.

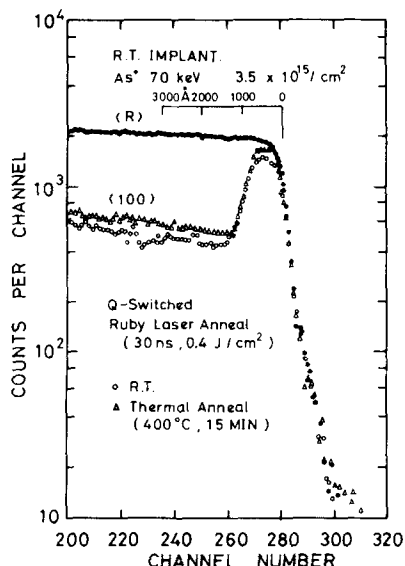


FIG. 3. RBS spectra of two kinds of Si annealed by Q-switched ruby laser.

mal energy. We will consider what happens as temperature rises. As to (1), since the gap E_g decreases with temperature, the optical absorption coefficient α increases. As to (2), since E_g decreases with temperature, a relaxation mechanism of hot electrons and holes within intrabands becomes a main process which is considered to have a relaxation time less than a psec¹⁵ (i.e., absorbed laser energy is transferred into thermal energy in a time less than a psec). As to (3), thermal diffusivity shows strong decrease with temperature. Therefore, by the positive feedback due to the above-mentioned effect in the three processes an initial fraction E_s of laser pulse energy increases the temperature of the irradiated-solid surface within absorption length α^{-1} which decreases at an accelerated rate with time.⁶ Once the liquid layer is formed, the other fraction E_l of laser pulse energy makes the liquid Si layer grow with time.^{2,8,9} The crystalline-recovery ratio in Fig. 1 is considered to be nearly equal to $E_l / (E_s + E_l)$, where $(E_s + E_l)$ is the absorbed energy.

In conclusion, since the spin density is strongly correlated with the optical absorption coefficient, from our ex-

perimental results and the above-mentioned discussion the initial absorption coefficient is a very important factor which dominates the effect of laser annealing. That is also the case even if there is a nonlinear absorption mechanism for the high power used for laser annealing. The spin density was found to yield a good criterion for predicting the effect of pulsed laser annealing of both amorphous Si and heavily damaged crystalline Si, especially in the case of Nd:YAG laser irradiation.

We would like to thank Dr. P. H. Kim, Dr. Y. Aoyagi, and Dr. Y. Segawa for cooperation on laser irradiation, and Professor S. Nakai and Dr. M. Matoba for lending the Q-switched ruby laser.

¹For example: R.T. Young, C.W. White, G.J. Clark, J. Narayan, W.H. Christie, M. Murakami, P.W. King, and S.D. Kramer, *Appl. Phys. Lett.* **32**, 139 (1978); G.K. Celler, J.M. Poate, and L.C. Kimerling, *ibid.* **32**, 464 (1978).

²T.N.C. Venkatesan, J.A. Golovchenko, J.M. Poate, P. Cowan, and G.K. Celler, *Appl. Phys. Lett.* **33**, 429 (1978).

³G.E.J. Eggermont, Y. Tamminger, and W.K. Hofker, *AIP Conf. Proc.* **50**, 321 (1978).

⁴J.C. Bean, H.J. Leamy, J.M. Poate, G.A. Rozgonyi, J.P. Van der Ziel, and J.S. Williams (unpublished).

⁵M. Miyao, M. Tamura, and T. Tokuyama, *Appl. Phys. Lett.* **33**, 828 (1978).

⁶M. Von Allmen, W. Luthy, J.P. Thomas, M. Fallavier, J.M. Mackowski, R. Kirsch, M.A. Nicolet, and M.E. Raulet, *Appl. Phys. Lett.* **34**, 82 (1979).

⁷G. Foti, E. Rimini, M. Bertolotti, and G. Vitali, *Phys. Lett. A* **430** (1978).

⁸D.H. Auston, C.M. Sarko, T.N.C. Venkatesan, R.E. Slusher, and J.A. Golovchenko, *Appl. Phys. Lett.* **33**, 437 (1978); Ref. 3, p. 11.

⁹K. Murakami, K. Gamo, S. Namba, M. Kawabe, Y. Aoyagi, and Y. Aka-saka, *Phys. Lett.* **70A**, 332 (1979); Ref. 3, p. 61.

¹⁰N.H. Brodsky, D.M. Kaplan, and J.F. Ziegler, *Proc. XI Intern. Conf. on Phys. Semicon.*, Warsaw, 1972, p. 529 (unpublished).

¹¹N.F. Mott and E.A. Davis, *Electronic Processes in Non-Crystalline Materials* (Clarendon, Oxford, 1971), p. 272-323.

¹²K. Murakami, K. Masuda, K. Gamo, and S. Namba, in *Proc. 4th Intern. Conf. on Ion Implantation in Semiconductors*, Osaka, 1974, p. 533 (unpublished).

¹³A smaller depth, e.g., $R_p + \Delta R_p$ or R_p , would be more representative of the averaged spin density in layers implanted with relatively low doses ($\leq 1 \times 10^{15}/\text{cm}^2$).

¹⁴K. Murakami, E. Ikawa, T. Nonoue, K. Gamo, and S. Namba (unpublished).

¹⁵N. Bloembergen, Ref. 3, p.1.